Results in Chemistry 9 (2024) 101645

Contents lists available at ScienceDirect

Results in Chemistry

journal homepage: www.sciencedirect.com/journal/results-in-chemistry

New ALKBH2 and ALKBH5 inhibitors for treating glioblastoma

Mirko Rivara [a], Gabriella Nicolini [b,c,d,*], Alessio Malacrida [b,d], Francesca Re [c,d,e], Matteo Incerti [a], Giulia Russo [a], Valentina Zuliani [a]

[a] Food and Drug Department, University of Parma, Parco Area delle Scienze 27/A, 43124 Parma, PR, Italy
[b] School of Medicine and Surgery, Experimental Neurology Unit, University of Milano-Bicocca, Via Cadore 48, 20900 Monza, MB, Italy
[c] GBM-BI-TRACE (GlioBlastoMa-BIcocca-TRAnslational-CEnter), University of Milano-Bicocca, Italy
[d] NeuroMi, Milan Center for Neurosciences, Italy
[e] School of Medicine and Surgery, Clinical Nanobiochemistry Lab, University of Milano-Bicocca, Via Cadore 48, 20900 Monza, MB, Italy

ARTICLE INFO

Keywords:
Brain cancer
Glioblastoma
ALKBH2 inhibitors
ALKBH5 inhibitors

ABSTRACT

Purpose: Glioblastoma is an aggressive brain tumor with high mortality and a median survival of about 15 months. Starting from our previous published compound, MV1035 that inhibited migration and invasiveness of glioblastoma U87 cells, and also exhibited a synergic effect in combination with the alkylating agent Temozolomide, we identified new active molecules, with the aim to understand the key motifs responsible for MV1035 activity against the DNA repair protein ALKBH2 and the RNA demethylase ALKBH5.
Materials and methods: We modified the original structure of MV1035, synthesizing new molecules that have been tested through MTT assay, cell-free ALKBH2 assay and cell-free ALKBH5 assay.
Results: We found that compound **6** is able to reduce the activity of both ALKBH2 and ALKBH5.
Conclusion: We obtained important information about the key motifs responsible for the activity of these inhibitors. However, considering the complexity, heterogeneity and plasticity of GBM and GSC cells, the new identified compound will need to be validated *in vivo*.

Introduction

Glioblastoma (GBM) is the most aggressive and deadly adult brain tumor and the development of a new therapeutic strategy for its treatment represents one of the millennium challenges.

The World Health Organization (WHO) Classification of Tumors of the Central Nervous System (CNS) [1], published in 2021, includes significant updates and refinements in the classification of glioblastoma, which is categorized primarily based on histological and molecular features in two major types: Glioblastoma IDH-wild type (WHO Grade 4) and Glioblastoma IDH-mutant (WHO Grade 4). Additionally, the WHO 2021 classification recognizes additional subtypes based on specific molecular features [1].

Despite considerable efforts to develop new therapeutic approaches [2,3], still today, after about 20 years, the standard treatment for newly diagnosed GBM contemplates surgical resection followed by post-operative focal conformal radiotherapy (RT) and chemotherapy based on the alkylating agent temozolomide (TMZ) and 6 cycles of adjuvant TMZ (Stupp regimen) [4,5].

However, GBM recurrence is inevitable and patients treated with standard therapy have a median survival of about 15 months [6].The reasons for this very high mortality are various, including inter- and intra-tumor heterogeneity, drug resistance, very high invasiveness, and very intricate interaction between GBM (principally glioblastoma stem cells, GSCs) and tumor microenvironment (including immune cells, blood vessels, astrocytes and extracellular matrix) [7–10].

As part of a multi-disciplinary study in which we tested potential antitumor molecules, we demonstrated that MV1035 molecule can inhibit the migration and invasiveness of glioblastoma U87 cells [11]. Moreover, through *in silico* analysis (SPILLO-PBS software) and cell free studies we identified the imidazobenzoxazin-5-thione (ALKBH5) as the direct target inhibited by MV1035.

Interestingly, MV1035 has also a synergic effect in combination with TMZ both on U87 and on patient-derived (PD) GSCs [12] and we demonstrated, according to a further *in silico* analysis, that its effect is also due to inhibition of alkylated DNA repair protein 2 (ALKBH2).

* Corresponding author at: School of Medicine and Surgery, University of Milano-Bicocca, Via Cadore 48, 20900 Monza, MB, Italy.
E-mail addresses: mirko.rivara@unipr.it (M. Rivara), gabriella.nicolini@unimib.it (G. Nicolini), alessio.malacrida@unimib.it (A. Malacrida), francesca.re1@unimib.it (F. Re), matteo.incerti@unipr.it (M. Incerti), giulia.russo@unipr.it (G. Russo), valentina.zuliani@unipr.it (V. Zuliani).

https://doi.org/10.1016/j.rechem.2024.101645
Received 20 May 2024; Accepted 4 July 2024
Available online 6 July 2024

Moreover, in the PD GCS7 cell line, MV1035 has proven to be effective inducing methylation of O6-methylguanine-DNA methyltransferase (MGMT) promoter and consequently reducing MGMT protein expression.

Considering MV1035′s ability to inhibit both ALKBH5 (crucial for maintaining GSCs tumorigenicity), [13] and ALKBH2 (involved in TMZ resistance) [14,15] this compound was considered a good candidate to be further developed.

Starting from MV1035 we modified the original structure with the aim to identify the key motifs that are responsible for its activity against the DNA repair protein ALKBH2 and the RNA demethylase ALKBH5 to gather information eventually leading to more potent inhibitors (see Fig. 1).

The new molecules were designed using the putative interactions between MV1035 and ALKBH5 found in our previous work without any molecular modeling help since, in this initial phase of the work, we prioritize the rapid exploration of some key features of MV1035 considering the chemical accessibility the number one priority. As previously stated MV1035 partially overlaps to the binding site of 2-oxoglutarate, this implies a competition for the same binding region, leading to the inhibition of the catalytic activity of ALKBH5. We considered two main structural components of the hit MV1035 (the tricyclic scaffold and the side chains), working then on the group in ortho position of the phenyl ring. As shown by our previous results the tricyclic moiety seems important for the interaction of MV1035 in its putative binding pocket while the propyl chain attached to the imidazole ring appeared to concede some space to work on.

Based on these observations we modified both the tricyclic imidazobenzoxazine original core and the alkyl chains connected to the imidazole ring (Fig. 2).

We synthesized compounds **1** and **2**, where the original side chains have been substituted with a shorter methyl group (**1**) and a longer methyl propanoate chain along with the elimination of the methyl group in the adjacent position (**2**). Compounds **1** and **2** were designed to investigate the effect that a change in the length of the aliphatic substituents on the heterocycle would have on the activity.

We also synthesized compound **3**, where the thiocarbonyl had been replaced with a carbonyl group, with the aim to understand if the presence of an oxygen atom instead of a sulfur one could influence the activity.

At the same time, we proceed to open the original tricyclic scaffold. In fact, another important aspect to clarify is the role of this central core. And we thought it could be evaluated both by opening it and by subsequently varying the substituents on the phenyl ring. Thus, we synthesized compounds **4** and **5**, keeping both the original side chains (methyl and propyl) (**4**) and the new longer one (methyl propanoate) (**5**). The central ring opening resulted in an o-methoxy 2-phenylimidazole scaffold.

We further modified this opened scaffold removing the methyl group from the methoxy on the phenyl ring, thus resulting in the phenolic derivatives **6**, **7** and **8**. This modification was considered as an intermediate structure between the original tricyclic system and the newly opened ones, where the phenolic group could eventually make an intramolecular hydrogen bond.

At last, after the preliminary results, we decided to replace the OH group of compound **6** with a carboxylic one (**9**), to test if the increased acidity could benefit the activity.

Material and methods

Chemistry

Microwave assisted synthesis was performed using a CEM Microwave Synthesizer—Discover Model 2.0. The final products were analyzed on a ThermoQuest (Italia) FlashEA 1112 Elemental Analyzer, for C, H, N. The percentages recorded were within ±0.4 % of the theoretical values. All products were also characterized by ^{1}H NMR and ^{13}C NMR. The ^{1}H NMR and ^{13}C NMR spectra were recorded on a Bruker 400 Avance spectrometer (400 MHz); chemical shifts (δ scale) are reported in parts per million (ppm) relative to the central peak of the solvent. ^{1}H NMR spectra are reported in order: multiplicity and number of protons; signals were characterized as s (singlet), dd (doublet of doublet), t

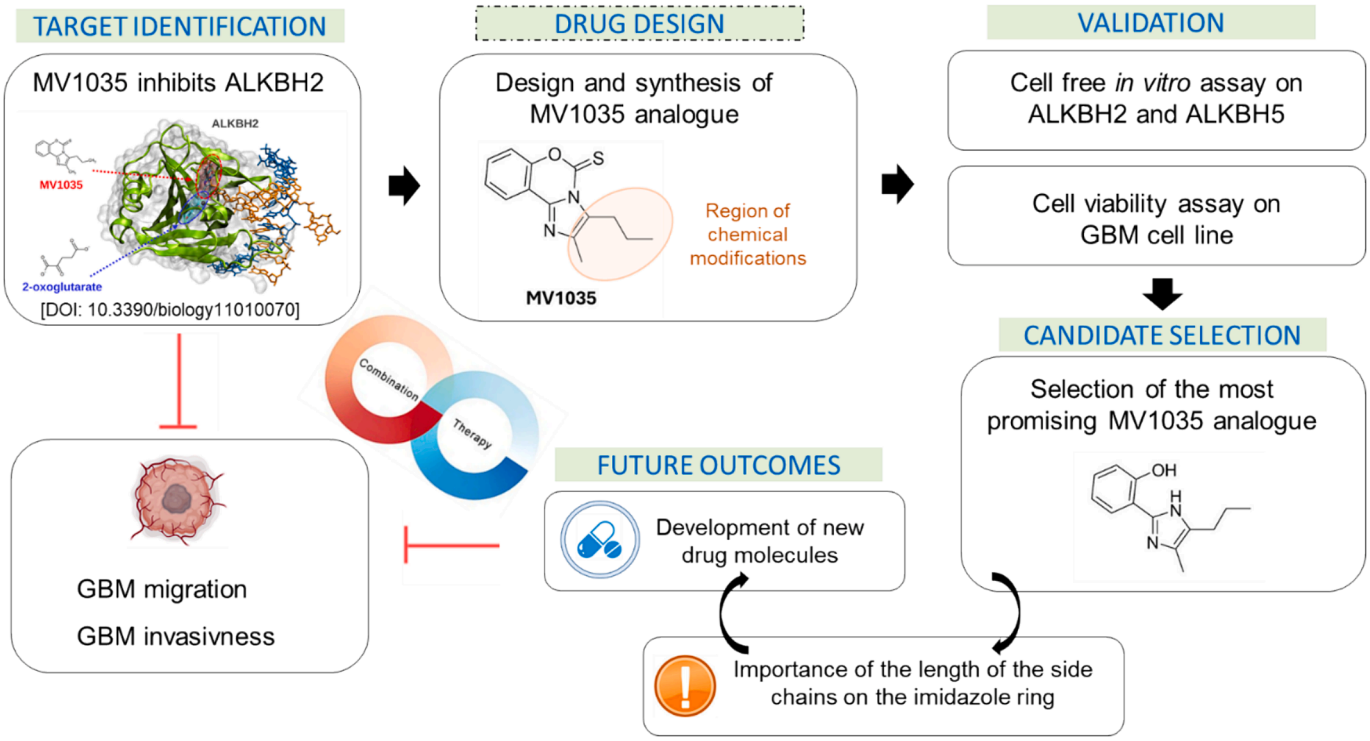

Fig. 1. Integrated drug discovery workflow adopted.

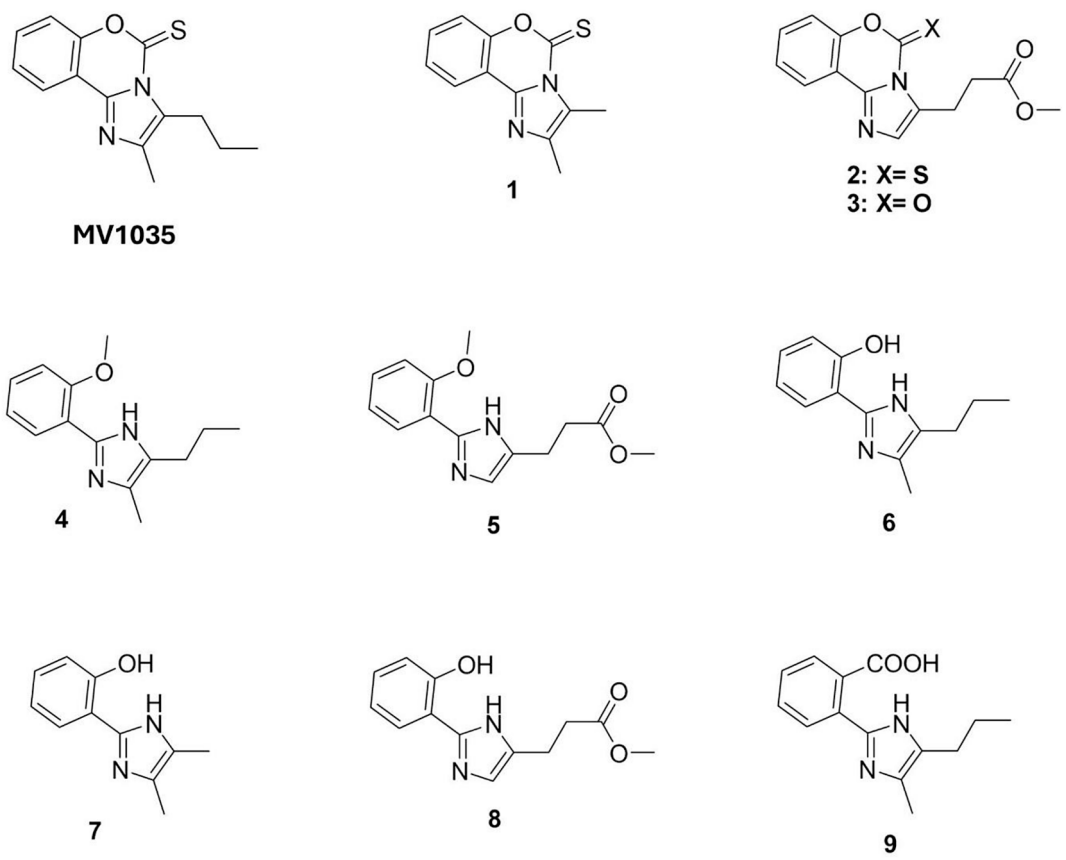

Fig. 2. Chemical structures of the compounds **1–9** and of the hit MV1035.

(triplet), m (multiplet). The ^{13}C NMR spectra were recorded at 100 MHz. Mass spectra were recorded on a single quadrupole analyzer Adivion Expression-L Compact Mass Spectrometer.

NMR-spectra (^{1}H NMR and ^{13}C NMR) of target compounds **1–9** are available in the Supplementary Information.

General procedure for the synthesis of compounds 1, 2 and 3

Compounds **1, 2** and **3** were prepared following the already published method [17] with slight modifications (for details and spectra see Supporting Information).

A solution of hydroxyphenyl-imidazole (0.80 mmol) and 1,1′-carbonyldiimidazole (CDI) or 1,1′-thiocarbonyldiimidazole (TCDI) (1.00 mmol) in 2 mL THF was placed in a sealable 10 mL microwave vial. The mixture was irradiated for 20 min, following a multistep method: 1 min setting the temperature at 70 °C (power 100 W, air cooling 2 bar) followed by 19 min at 90 °C (power 200 W, air cooling 2 bar). After the removal of the solvent the residue was purified by flash chromatography (SiO_2, DCM/Petroleum ether = 1:1).

2,3-dimethyl-5H-benzo[e]imidazo[1,2-c][1,3]oxazine-5-thione (**1**). White solid; Yield: 68 %; ^{1}H NMR (400 MHz, CDCl3) δ = 8.16 (d, 1H), 7.52 (t, 1H), 7.40 (m, 2H), 6.90 (t, 1H), 2.79 (s, 3H), 2.33 (s, 3H); ^{13}C NMR (100 MHz, CDCl3) δ = 175.46, 151.10, 140.07, 137.65, 130.93, 126.38, 124.80, 123.12, 115.89, 113.49, 13.72, 13.19; APCI, [M + H] +): 231; C,H,N: C_{calc} 62.59 %, C_{found} 62.38 %, H_{calc} 4.38 %, H_{found} 4.45 %, N_{calc} 12.16 %, N_{found} 12.02 %.

methyl 3-(5-oxo-5H-benzo[e]imidazo[1,2-c][1,3]oxazin-2-yl)propanoate (**2**). White solid; Yield: 71 %; ^{1}H NMR (400 MHz, CDCl3) δ = 8.19 (d, 1H), 7.58 (t, 1H), 7.49 (s, 1H), 7.44 (m, 2H), 3.72 (s, 3H), 3.08 (t, 2H), 2.81 (t, 2H); ^{13}C NMR (100 MHz, CDCl3) δ = 173.11, 150.32, 145.05, 142.78, 132.01, 126.30, 123.37, 117.19, 111.84, 51.91, 32.71, 23.70; APCI, [M + H] +): 273; C,H,N: C_{calc} 61.76 %, C_{found} 61.99 %, H_{calc} 4.44 %, H_{found} 4.54 %, N_{calc} 10.29 %, N_{found} 10.52 %.

methyl 3-(5-thioxo-5H-benzo[e]imidazo[1,2-c][1,3]oxazin-2-yl) propanoate (**3**). White solid; Yield: 59 %; ^{1}H NMR (400 MHz, CDCl3) δ = 8.21 (d, 1H), 7.79 (t, 1H), 7.61 (s, 1H), 7.50 (m, 2H), 3.74 (s, 3H), 3.08 (t, 2H), 2.83 (t, 2H); ^{13}C NMR (100 MHz, CDCl3) δ = 173.04, 151.50, 146.48, 138.26, 132.35, 127.31, 123.57, 116.89, 114.94, 51.92, 32.53, 23.77; APCI, [M + H] +): 289; C,H,N: C_{calc} 58.32 %, C_{found} 58.11 %, H_{calc} 4.20 %, H_{found} 4.51 %, N_{calc} 9.72 %, N_{found} 10.01 %.

General procedure for the synthesis of compounds 4, 5, 8 and 9

The compounds **4, 5, 8** and **9** were prepared following the already published method [17] with slight modifications (for details and spectra see Supporting Information).

To a solution of benzaldehyde (1.00 mmol) in MeOH (3 mL) was added NH_4COOCH_3 (5.00 mmol) followed by the addition of a solution of dicarbonyl compound (1.00 mmol) in MeOH (3 mL). The resulting mixture was stirred at room temperature (r.t.) overnight.

The methanol was then evaporated under reduced pressure and the residue quenched with a saturated aqueous solution of $NaHCO_3$ and extracted three times with EtOAc. The organic layers were collected and dried over anhydrous Na_2SO_4 and evaporated under reduced pressure.

The residue was purified by flash chromatography (SiO_2, DCM/EtOAc = 20:1). Compounds **4, 5, 8** and **9** were then crystallized as hydrochloride from abs EtOH and anhydrous Et_2O.

2-(2-methoxyphenyl)-4-methyl-5-propyl-1H-imidazole hydrochloride (**4**). White solid; Yield: 77 %; ^{1}H NMR (400 MHz, DMSO-d_6) δ = 7.97 (d, 1H), 7.59 (t, 1H), 7.29 (d, 1H), 7.16 (t, 1H), 3.96 (s, 3H), 2.64 (t, 2H), 2.29 (s, 3H) 1.63 (m, 2H), 0.91 (t, 3H); ^{13}C NMR (100 MHz, DMSO-d_6) δ = 156.80, 138.79, 133.70, 129.62, 125.62, 121.42, 112.87, 112.17, 56.57, 25.17, 22.67, 13.72, 9.29; APCI, [M + H] +): 231; C,H, N: C_{calc} 63.03 %, C_{found} 62.88 %, H_{calc} 7.18 %, H_{found} 7.51 %, N_{calc} 10.50 %, N_{found} 10.21 %.

methyl 3-(2-(2-methoxyphenyl)-1H-imidazol-5-yl)propanoate

hydrochloride (**5**). White solid; Yield: 53 %; ^{1}H NMR (400 MHz, DMSO-d_6) δ = 8.00 (d, 1H), 7.62 (t, 1H), 7.48 (s, 1H), 7.32 (d, 1H), 7.19 (t, 1H), 3.98 (s, 3H), 3.63 (s, 3H), 2.98 (t, 2H), 2.81 (t, 2H); ^{13}C NMR (100 MHz, DMSO-d_6) δ = 172.68, 156.95, 140.39, 134.09, 133.22, 129.44, 121.53, 116.75, 113.00, 111.82, 56.58, 52.05, 32.39, 20.18; APCI, [M + H] +): 261; C,H,N: C_{calc} 56.67 %, C_{found} 57.02 %, H_{calc} 5.77 %, H_{found} 5.63 %, N_{calc} 9.44 %, N_{found} 9.62 %.

methyl 3-(2-(2-hydroxyphenyl)-1H-imidazol-5-yl)propanoate hydrochloride (**8**). White solid; Yield: 49 %; ^{1}H NMR (400 MHz, DMSO-d_6) δ = 8.01 (d, 1H), 7.44 (t, 1H), 7.39 (s, 1H), 7.23 (d, 1H), 7.03 (t, 1H), 3.62 (s, 3H), 2.98 (t, 2H), 2.81 (t, 2H); ^{13}C NMR (100 MHz, DMSO-d_6) δ = 172.72, 156.03, 141.19, 133.60, 132.86, 128.78, 120.16, 117.28, 116.44, 110.17, 52.03, 32.46, 20.17; APCI, [M + H] +): 247; C,H,N: C_{calc} 55.23 %, C_{found} 55.52 %, H_{calc} 5.35 %, H_{found} 5.13 %, N_{calc} 9.91 %, N_{found} 10.12 %.

2-(4-methyl-5-propyl-1H-imidazol-2-yl) benzoic acid hydrochloride (**9**). White solid; Yield: 70 %; ^{1}H NMR (400 MHz, DMSO-d_6) δ = 8.16 (d, 1H), 7.92 (d, 1H), 7.65 (t, 1H), 7.50 (t, 1H), 2.54 (t, 2H), 2.22 (s, 3H) 1.61 (m, 2H), 0.91 (t, 3H); ^{13}C NMR (100 MHz, DMSO-d_6) δ = 168.42, 142.34; 133.94, 133.16, 131.60, 131.29, 129.54, 127.89, 126.63, 125.76, 26.39, 22.60, 13.88, 10.06; APCI, [M + H] +): 245; C,H,N: C_{calc} 59.89 %, C_{found} 59.68 %, H_{calc} 6.10 %, H_{found} 6.24 %, N_{calc} 9.98 %, N_{found} 9.72 %.

General procedure for the synthesis of compounds 6 and 7

The compounds **6** and **7** were prepared following the already published method [16] with slight modifications (for details and spectra see Supporting Information).

A solution of methoxyphenyl-imidazole (0.6 mmol) in 48 % HBr (2 mL) was placed in a sealable 10 mL microwave vial. The mixture was irradiated for 8 min, following a multistep method: 1 min setting the temperature at 120 °C (power 100 W, air cooling 2 bar) followed by 7 min at 160 °C (power 130 W, air cooling 2 bar). The reaction mixture was quenched with a saturated aqueous solution of $NaHCO_3$ and extracted three times with EtOAc. The organic layers were collected and dried over anhydrous Na_2SO_4 and evaporated under reduced pressure. The residue was purified by flash chromatography (SiO_2, DCM/EtOAc = 20:1). Compounds **6** and **7** were then crystallized as hydrochloric salts from abs EtOH and anhydrous Et_2O.

2-(4-methyl-5-propyl-1H-imidazol-2-yl)phenol hydrochloride (**6**). White solid; Yield: 62 %; ^{1}H NMR 10(400 MHz, DMSO-d_6) δ = 7.87 (d, 1H), 7.43 (t, 1H), 7.19 (d, 1H), 7.02 (t, 1H), 2.63 (t, 2H), 2.28 (s, 3H) 1.63 (m, 2H), 0.90 (t, 3H); ^{13}C NMR (100 MHz, DMSO-d_6) δ = 155.81, 139.68, 133.29, 129.30, 128.79, 125.32, 120.10, 117.17, 110.54, 25.20, 22.26, 13.71, 9.29; APCI, [M + H] +): 217; C,H,N: C_{calc} 61.78 %, C_{found} 61.52 %, H_{calc} 6.78 %, H_{found} 6.45 %, N_{calc} 11.08 %, N_{found} 11.36 %.

2-(4,5-dimethyl-1H-imidazol-2-yl)phenol hydrochloride (**7**). White solid; Yield: 72 %; ^{1}H NMR (400 MHz, DMSO-d_6) δ = 7.81 (d, 1H), 7.24 (t, 1H), 6.98 (d, 1H), 6.90 (t, 1H), 2.18 (s, 6H); ^{13}C NMR (100 MHz, DMSO-d_6) δ = 156.43, 142.45, 130.59, 125.98, 125.63, 119.37, 117.06, 112.86, 10.31; APCI, [M + H] +): 189; C,H,N: C_{calc} 58.80 %, C_{found} 58.99 %, H_{calc} 5.83 %, H_{found} 6.02 %, N_{calc} 12.47 %, N_{found} 12.21 %.

Cytotoxicity: MTT assay

U87-MG cells viability was assessed using MTT assay. Cells were seeded in 96-well plates at a density of 5 x 10^3 cells/well. Cells were treated with MV1035 or compounds 1–9 (50 μM). Only compound 6 was assessed also at 10 and 25 μM concentrations. Following 24, 48, and 72 h of incubation, MTT assay was conducted. MTT solution (3-(4,5-dimethylthiazol-2-yl)-2,5-diphenyltetrazolium bromide) was directly added to culture medium to achieve a final concentration of 0.5 mg/mL. After 4 h of incubation, plates were centrifuged at 1000 x *g* for 10 min, supernatant was removed, and formazan crystals were dissolved in acidified 2-propanol. Absorbance readings were taken at 570 nm using a microplate reader (BMG Labtech, Ortenberg, Germany).

ALKBH2 activity assay

DNA demethylation activity of ALKBH2 was evaluated by cell-free assay. 0.6 μg/μL of active recombinant ALKBH2 protein (Active Motif, Carlsbad, CA, USA) were incubated with 1 μg/50 μL of methylated single-stranded DNA (ssDNA) sequence (50-AAAGCAG(1-mA)ATTC-GAAAAAGCGAAA-30; Ella Biotech, Fürstenfeldbruck, Germany). The reaction was conducted with or without MV1035 or compounds 1–9 in buffer containing 50 mM Hepes pH 8.0, 50 μM Fe(NH4)2(SO4)2, 1 mM 2-oxoglutarate, and 2 mM ascorbic acid. Following 30 min of incubation at 37 °C, the reaction was heat-inactivated at 95 °C for 5 min. Subsequently, the resulting ssDNA was mixed with equimolar amounts of complementary unmethylated ssDNA (1 μg/50 μL, 30-TTTCGTCTTAAGCTTTTTCGCTTT-50). The annealing reaction between the two ssDNA sequences was carried out in a thermal cycler with the following conditions: 2 min at 95 °C, 45 min at 25 °C, and 5 min at 4 °C. After annealing, the DNA was digested with EcoRI restriction enzyme: DNA was incubated at 37 °C for 45 min with EcoRI buffer and EcoRI restriction enzyme, following the manufacturer's instructions (Thermofisher, Waltham, MA, USA). EcoRI was then heat-inactivated at 65 °C for 20 min. Digested and undigested DNA samples were separated on a native polyacrylamide gel. Finally, DNA was stained with SYBR Safe and visualized using Amersham Imager 600.

ALKBH5 activity assay

RNA demethylation activity of ALKBH5 was assessed by cell-free assay. In a microtube, 4 μM of active recombinant ALKBH5 protein (Active Motif, Carlsbad, CA, USA), 80 μM of M6A-ssRNA (GG-m6A-CU; Ella Biotech, Fürstenfeldbruck, Germany), 150 μM of α-ketoglutarate, 150 μM of ammonium iron sulfate hexahydrate, 2 mM of L-ascorbate, and 50 mM of Hepes pH 7.5 (Sigma Aldrich, USA) were combined and incubated with or without MV1035 or compounds 1–9 at 4 °C for 30 min. Subsequently, 5 μL of the reaction solution were spotted onto a nylon membrane, and dot blot against m6A-RNA was carried out following the manufacturer's instructions. Primary antibody against m6A-RNA (1:250, Sigma Aldrich, USA) and secondary antibody anti-mouse (1:2000, Jackson Immuno Research, UK) were employed. Dot blot was then visualized using Amersham Imager 600.

Statistical analysis

Data are reported as average ± standard deviation (SD) from at least three independent experiments. Statistical analysis was performed using GraphPad Prism 8 software. The differences between control and treated cells were evaluated using One Way ANOVA analysis of variance followed by Dunnett's multiple comparison test. Statistical significance was set at $p < 0.05$ or 0.01.

Results and discussion

Chemistry

Here are reported the synthetic routes for target compounds **1–9** (Scheme 1. Scheme 2. Scheme 3. Scheme 4). All the target molecules

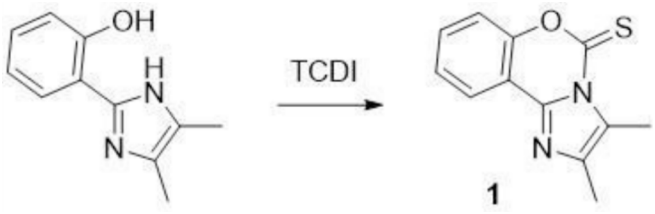

Scheme 1. Synthesis of compound **1**.

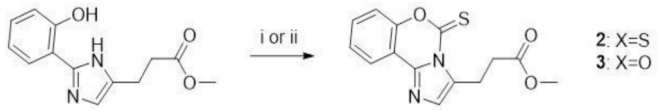

Scheme 2. Synthesis of compounds **2** and **3**: i: TCDI (for compound **2**); ii: CDI (for compound **3**).

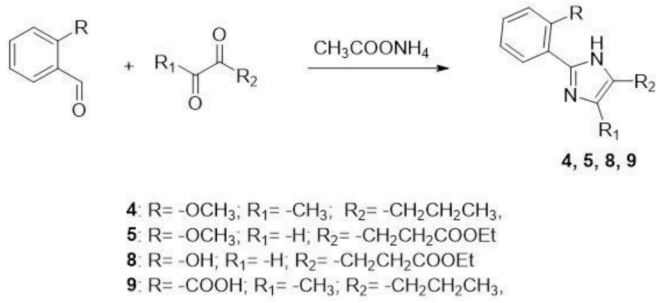

Scheme 3. Synthesis of compounds **4**, **5**, **8** and **9**.

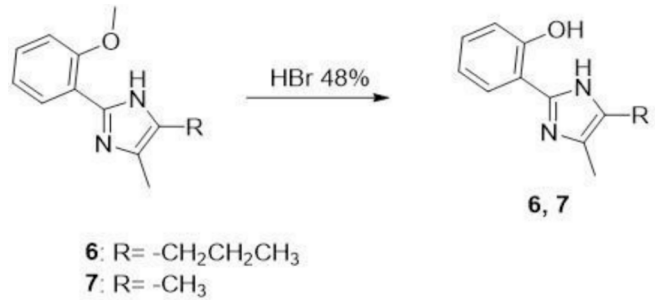

Scheme 4. Synthesis of compounds **6** and **7**.

were obtained in good yields and checked for structure confirmation and purity before testing.

Citotoxicity assay

U87-MG cells were treated with MV1035 or compounds **1**–**9** (50 μM). After 24, 48 and 72 h of treatment, MTT assay was performed to assess cell viability (Fig. 3).

Compound **2** did not perturb cell viability of U87-MG cells at any time point considered. U87 cell viability was slightly reduced by compounds **3**, **4** and **5** only at 72 h, and by compounds 7 and **9** at 48 and 72 h. Compounds **1**, **6** and **8** had a significant time-dependent effect at all time points considered. Among these, compound **6** was the most effective in reducing the viability of U87-MG cells.

ALKBH2 activity cell-free assay

Inhibition of active recombinant ALKBH2 protein by MV1035 or compounds **1**–**9** was evaluated by cell-free ALKBH2 activity assay. Methylated ssDNA oligonucleotide was incubated with ALKBH2 alone or with MV1035 or compounds **1**–**9** (50 μM). After annealing with a complementary ssDNA oligonucleotide, DNA was digested with EcoRI restriction enzyme (Fig. 4).

In untreated CTRL, DNA is partially digested by ALKBH2. Compounds **2** and **3** were unable to inhibit ALKBH2 activity and the results are comparable to untreated CTRL. Compounds **1**, **4**, **5**, **7** and **9** reduced ALKBH2 activity significantly, but less than 50 %. Compound **8** significantly reduced the activity of ALKBH2 by approximately 50 %, while Compound **6** was once again the most effective compound, significantly reducing the activity of ALKBH2 by approximately 75 %.

ALKBH5 activity cell-free assay

Inhibition of active recombinant ALKBH5 by MV1035 or compounds **1**–**9** was evaluated by dot blot analysis. ALKBH5 protein was mixed with m6A-RNA alone or with MV1035 or compounds **1**–**9** (50 μM concentration) (Fig. 5).

Compounds **2**, **3** and **9** did not inhibit which was comparable to untreated CTRL. Compounds **4** and **5** induced a slight and non-significant ALKBH5 inhibition, while compounds **1**, **6**, **7** and **8** significantly inhibited the demethylase activity, increasing the signal obtained in dot-blot assay. Once again, compound **6** was found to be the most effective compound.

Deepening the effects of compound 6

Compound **6** was found to be the most effective counteracting the viability of U87-MG cells and in inhibiting the activity of the DNA repair protein ALKBH2 and the RNA demethylase ALKBH5. For this reason, it was decided to further investigate its effect by evaluating different concentrations.

- MTT assay (Fig. 6): U87-MG cells were treated with compound **6** at 10, 25 and 50 μM concentration for 24, 48 and 72 h. The effect against cell viability was dose and time dependent.
- ALKBH2 cell-free assay (Fig. 7A): methylated ssDNA oligonucleotide was incubated in the presence of ALKBH2 alone or with compound **6** at 10, 25 and 50 μM concentrations. ALKBH2 inhibition by compound **6** was dose dependent, with an IC50 of approximately 25 μM.

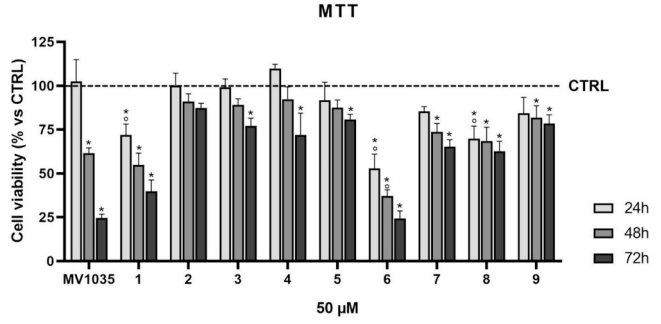

Fig. 3. U87 cells viability treated with MV1035 or compounds **1**–**9** (50 μM) for 24, 48 and 72 h. Graphs represent mean percentage ± SD of cell viability compared to untreated controls, arbitrarily set to 100 %. *p < 0.01 vs control, °p < 0.01 vs MV1035.

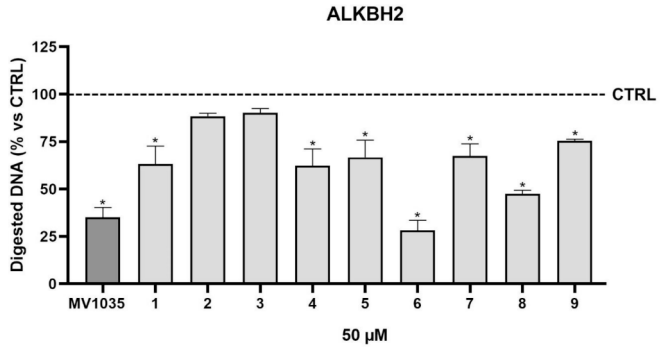

Fig. 4. Cell-free ALKBH2 demethylase activity assay in presence of MV1035 or compounds **1**–**9** (50 μM). Data are represented as mean percentage ± SD of digested DNA compared to untreated controls, arbitrarily set to 100 %. *p < 0.01 vs. CTRL.

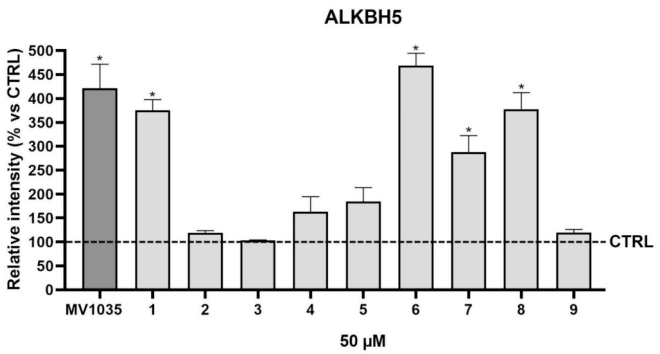

Fig. 5. Cell-free dot blot analysis of ALKBH5 demethylase activity in presence of MV1035 or compounds **1**–**9** (50 μM). Data are represented as the average percentage ± SD compared to controls, arbitrarily set to 100 %. *p < 0.01.

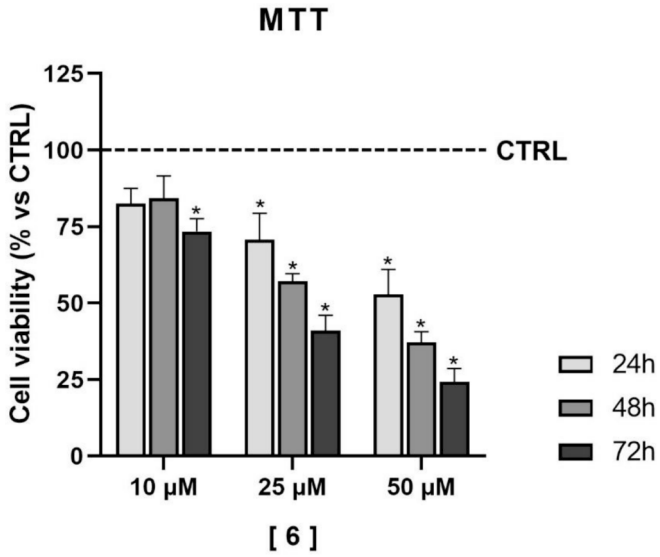

Fig. 6. Cell viability of U87-MG cells treated with different concentrations of compound **6** (10, 25 and 50 μM) for 24, 48 and 72 h. Graphs represent mean percentage ± SD of cell viability compared to untreated controls, arbitrarily set to 100 %. *p < 0.01 vs control.

- ALKBH5 cell-fee assay: (Fig. 7B): ALKBH5 protein was mixed with m6A-RNA alone or with compound **6** at 10, 25 and 50 μM concentrations. ALKBH2 inhibition by compound **6** was significantly dose dependent.

Conclusion

A set of molecules obtained modifying the previous lead compound MV1035 have been synthesized and tested as anti-tumor agents, with the aim to understand the structural features of the parental compound responsible for the activity against the DNA repair protein ALKBH2 and the RNA demethylase ALKBH5.

The results highlight the importance of the length of the side chains on the imidazole ring. In fact, elongating the side chain by inserting a propanoate is always detrimental for the activity (compounds **2**, **3**, **5** and **8**), while the presence of two methyl groups is better tolerated, even if the molecules obtained (compounds **1** and **7**) are less active than the lead MV1035.

These results demonstrate that a propyl and a methyl on the imidazole ring are critical.

Considering the opening of the original tricyclic scaffold, the results highlight how this modification is well tolerated, as long as the hydroxyl group is maintained. In fact, compound **6** proved to be the best one in all the tests carried out, also showing a dose-dependent activity in the MTT assay and in the ALKBH2 and ALKBH5 cell-free assays. In all the tests performed, compound **6** proved to be even more active than the lead MV1035, thus allowing us to understand the key motifs responsible for the activity of these inhibitors, and to identify a new potent molecule, which will be a novel starting point for further studies.

Considering the complexity, heterogeneity and plasticity of GBM and GSC cells, it is difficult to predict and identify effective drug targets. Moreover, *in vitro* models may not fully replicate the *in vivo* environment thus the new identified compound 6 will need to be validated in animal models. Moreover, the identification of the key motifs responsible for the activity of MV1035 will open the possibility to design new compounds with improved efficacy and selectivity.

CRediT authorship contribution statement

Mirko Rivara: Writing – original draft, Supervision, Methodology, Investigation, Data curation, Conceptualization. **Gabriella Nicolini:** Writing – review & editing, Writing – original draft, Supervision, Funding acquisition, Data curation, Conceptualization. **Alessio Malacrida:** Writing – original draft, Methodology, Investigation, Data curation. **Francesca Re:** Writing – review & editing, Conceptualization. **Matteo Incerti:** Investigation. **Giulia Russo:** Investigation. **Valentina Zuliani:** Writing – review & editing, Writing – original draft,

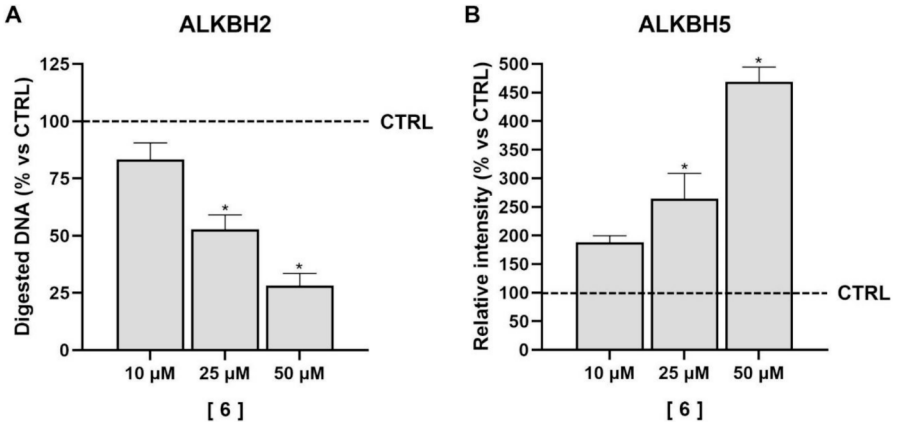

Fig. 7. Cell-free ALKBH2 (A) and ALKBH5 (B) demethylase activity assay in presence of different concentrations of compound **6**. Data are represented as mean percentage ± SD compared to untreated controls, arbitrarily set to 100 %. *p < 0.01 vs. CTRL.

Methodology, Investigation, Data curation, Conceptualization.

Declaration of competing interest

The authors declare that they have no known competing financial interests or personal relationships that could have appeared to influence the work reported in this paper.

Acknowledgments

This work was supported by Fondazione Giovanni Celeghin (www.fondazioneceleghin.it).

We thank Dr. Francesco Saverio Sica for his contribution in revising the manuscript.

Appendix A. Supplementary data

Supplementary data to this article can be found online at https://doi.org/10.1016/j.rechem.2024.101645.

References

[1] D.N. Louis, A. Perry, P. Wesseling, D.J. Brat, I.A. Cree, D. Figarella-Branger, C. Hawkins, H.K. Ng, S.M. Pfister, G. Reifenberger, R. Soffietti, A. von Deimling, D. W. Ellison, The 2021 WHO classification of tumors of the central nervous system: A summary, Neuro Oncol. 23 (2021) 1231–1251, https://doi.org/10.1093/neuonc/noab106.

[2] S. Kumari, R. Gupta, R.K. Ambasta, P. Kumar, Multiple therapeutic approaches of glioblastoma multiforme: From terminal to therapy, Biochim. Biophys. Acta 1878 (2023) 188913, https://doi.org/10.1016/j.bbcan.2023.188913.

[3] S.A. Rios, S. Oyervides, D. Uribe, A.M. Reyes, V. Fanniel, J. Vazquez, M. Keniry, Emerging therapies for glioblastoma, Cancers (Basel) 16 (2024) 1485, https://doi.org/10.3390/cancers16081485.

[4] R. Stupp, W.P. Mason, M.J. van den Bent, M. Weller, B. Fisher, M.J.B. Taphoorn, K. Belanger, A.A. Brandes, C. Marosi, U. Bogdahn, J. Curschmann, R.C. Janzer, S. K. Ludwin, T. Gorlia, A. Allgeier, D. Lacombe, J.G. Cairncross, E. Eisenhauer, R. O. Mirimanoff, European organisation for research and treatment of cancer brain tumor and radiotherapy groups, national cancer institute of Canada clinical trials group, radiotherapy plus concomitant and adjuvant temozolomide for glioblastoma, N. Engl. J. Med. 352 (2005) 987–996, https://doi.org/10.1056/NEJMoa043330.

[5] T. Gupta, J.M.P. Selvarajan, S. Kannan, N. Menon, A. Dasgupta, A. Chatterjee, Updated systematic review and meta-analysis of extended adjuvant temozolomide in patients with newly diagnosed glioblastoma, Neurooncol. Adv. 5 (2023) vdad086, https://doi.org/10.1093/noajnl/vdad086.

[6] L.R. Schaff, I.K. Mellinghoff, Glioblastoma and other primary brain malignancies in adults: A review, J. Am. Med. Assoc. 329 (2023) 574–587, https://doi.org/10.1001/jama.2023.0023.

[7] J.S. Castresana, B. Meléndez, Glioblastoma biology, genetics and possible therapies, Cells 12 (2023) 2063, https://doi.org/10.3390/cells12162063.

[8] R.D. Read, Z.M. Tapp, P. Rajappa, D. Hambardzumyan, Glioblastoma microenvironment-from biology to therapy, Genes Dev. 38 (2024) 360–379, https://doi.org/10.1101/gad.351427.123.

[9] C. Xu, P. Hou, X. Li, M. Xiao, Z. Zhang, Z. Li, J. Xu, G. Liu, Y. Tan, C. Fang, Comprehensive understanding of glioblastoma molecular phenotypes: classification, characteristics, and transition, Cancer Biol. Med. 21 (2024) 363–381, https://doi.org/10.20892/j.issn.2095-3941.2023.0510.

[10] Y.A. Yabo, D.H. Heiland, Understanding glioblastoma at the single-cell level: Recent advances and future challenges, PLoS Biol. 22 (2024) e3002640.

[11] A. Malacrida, M. Rivara, A. Di Domizio, G. Cislaghi, M. Miloso, V. Zuliani, G. Nicolini, 3D proteome-wide scale screening and activity evaluation of a new ALKBH5 inhibitor in U87 glioblastoma cell line, Bioorg. Med. Chem. 28 (2020) 115300, https://doi.org/10.1016/j.bmc.2019.115300.

[12] A. Malacrida, A. Di Domizio, A. Bentivegna, G. Cislaghi, E. Messuti, S.M. Tabano, C. Giussani, V. Zuliani, M. Rivara, G. Nicolini, MV1035 overcomes temozolomide resistance in patient-derived glioblastoma stem cell lines, Biology (Basel) 11 (2022) 70, https://doi.org/10.3390/biology11010070.

[13] S. Zhang, B.S. Zhao, A. Zhou, K. Lin, S. Zheng, Z. Lu, Y. Chen, E.P. Sulman, K. Xie, O. Bögler, S. Majumder, C. He, S. Huang, m6A demethylase ALKBH5 maintains tumorigenicity of glioblastoma stem-like cells by sustaining FOXM1 expression and cell proliferation program, Cancer Cell 31 (2017) 591–606.e6, https://doi.org/10.1016/j.ccell.2017.02.013.

[14] R. Gutierrez, T.R. O'Connor, DNA direct reversal repair and alkylating agent drug resistance, Cancer Drug Resist. 4 (2021) 414–423, https://doi.org/10.20517/cdr.2020.113.

[15] T.-C.-A. Johannessen, L. Prestegarden, A. Grudic, M.E. Hegi, B.B. Tysnes, R. Bjerkvig, The DNA repair protein ALKBH2 mediates temozolomide resistance in human glioblastoma cells, Neuro Oncol. 15 (2013) 269–278, https://doi.org/10.1093/neuonc/nos301.

[16] M. Fantini, V. Zuliani, M.A. Spotti, M. Rivara, Microwave assisted efficient synthesis of imidazole-based privileged structures, J. Comb. Chem. 12 (2010) 181–185, https://doi.org/10.1021/cc900152y.

[17] V. Zuliani, G. Cocconcelli, M. Fantini, C. Ghiron, M. Rivara, A practical synthesis of 2,4(5)-diarylimidazoles from simple building blocks, J. Org. Chem. 72 (2007) 4551–4553, https://doi.org/10.1021/jo070187d.